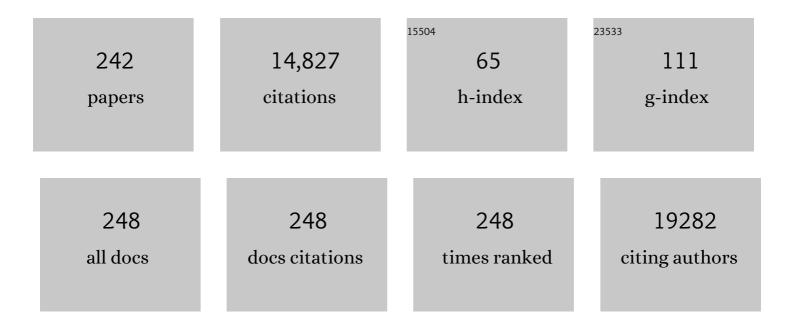
List of Publications by Year in descending order

Source: https://exaly.com/author-pdf/2696359/publications.pdf

Version: 2024-02-01



#	Article	IF	CITATIONS
1	Characterization of Irradiated Starches by Using FT-Raman and FTIR Spectroscopy. Journal of Agricultural and Food Chemistry, 2002, 50, 3912-3918.	5.2	923
2	Multiplex Biosensor Using Gold Nanorods. Analytical Chemistry, 2007, 79, 572-579.	6.5	477
3	Fluorescent Ag Clusters via a Protein-Directed Approach as a Hg(II) Ion Sensor. Analytical Chemistry, 2011, 83, 2883-2889.	6.5	400
4	Discriminant analysis of edible oils and fats by FTIR, FT-NIR and FT-Raman spectroscopy. Food Chemistry, 2005, 93, 25-32.	8.2	394
5	Infrared Heating in Food Processing: An Overview. Comprehensive Reviews in Food Science and Food Safety, 2008, 7, 2-13.	11.7	318
6	Surface-Enhanced Raman Spectroscopy Applied to Food Safety. Annual Review of Food Science and Technology, 2013, 4, 369-380.	9.9	305
7	Examination of Cholesterol oxidase attachment to magnetic nanoparticles. Journal of Nanobiotechnology, 2005, 3, 1.	9.1	264
8	CRISPR-dCas9 mediated TET1 targeting for selective DNA demethylation at <i>BRCA1</i> promoter. Oncotarget, 2016, 7, 46545-46556.	1.8	263
9	A mixed self-assembled monolayer-based surface plasmon immunosensor for detection of E. coli O157:H7. Biosensors and Bioelectronics, 2006, 21, 998-1006.	10.1	256
10	Nuclear Targeting Dynamics of Gold Nanoclusters for Enhanced Therapy of HER2 ⁺ Breast Cancer. ACS Nano, 2011, 5, 9718-9725.	14.6	246
11	Gold Nanorod Probes for the Detection of Multiple Pathogens. Small, 2008, 4, 2204-2208.	10.0	221
12	Gold Nanorod/Fe ₃ O ₄ Nanoparticle "Nanoâ€Pearlâ€Necklaces―for Simultaneous Targeting, Dualâ€Mode Imaging, and Photothermal Ablation of Cancer Cells. Angewandte Chemie - International Edition, 2009, 48, 2759-2763.	13.8	216
13	Epitaxial superlattices with titanium nitride as a plasmonic component for optical hyperbolic metamaterials. Proceedings of the National Academy of Sciences of the United States of America, 2014, 111, 7546-7551.	7.1	198
14	Magnetic and Gold-Coated Magnetic Nanoparticles as a DNA Sensor. Analytical Chemistry, 2006, 78, 3234-3241.	6.5	179
15	Comparison of near-infrared, fourier transform-infrared, and fourier transform-raman methods for determining olive pomace oil adulteration in extra virgin olive oil. JAOCS, Journal of the American Oil Chemists' Society, 2001, 78, 889.	1.9	166
16	Microscopic and Spectroscopic Evaluation of Inactivation of Staphylococcus aureus by Pulsed UV Light and Infrared Heating. Food and Bioprocess Technology, 2010, 3, 93-104.	4.7	166
17	Nanoscale Drug Delivery Systems: From Medicine to Agriculture. Frontiers in Bioengineering and Biotechnology, 2020, 8, 79.	4.1	164
18	Inactivation of <i>Staphylococcus aureus</i> in Milk Using Flowâ€Through Pulsed UVâ€Light Treatment System. Journal of Food Science, 2007, 72, M233-9.	3.1	160

#	Article	IF	CITATIONS
19	Multifunctional Magnetic–Optical Nanoparticle Probes for Simultaneous Detection, Separation, and Thermal Ablation of Multiple Pathogens. Small, 2010, 6, 283-289.	10.0	160
20	Current Technologies of Electrochemical Immunosensors: Perspective on Signal Amplification. Sensors, 2018, 18, 207.	3.8	157
21	Spectroscopic characterization of microorganisms by Fourier transform infrared microspectroscopy. Biopolymers, 2005, 77, 368-377.	2.4	156
22	Surface Modification of Cetyltrimethylammonium Bromide-Capped Gold Nanorods to Make Molecular Probes. Langmuir, 2007, 23, 9114-9119.	3.5	154
23	Surface-Enhanced Raman Scattering Based Nonfluorescent Probe for Multiplex DNA Detection. Analytical Chemistry, 2007, 79, 3981-3988.	6.5	153
24	Separation and detection of multiple pathogens in a food matrix by magnetic SERS nanoprobes. Analytical and Bioanalytical Chemistry, 2011, 399, 1271-1278.	3.7	153
25	A SERS DNAzyme biosensor for lead ion detection. Chemical Communications, 2011, 47, 4394.	4.1	150
26	Quantitative imaging of single mRNA splice variants in living cells. Nature Nanotechnology, 2014, 9, 474-480.	31.5	148
27	Identity Profiling of Cell Surface Markers by Multiplex Gold Nanorod Probes. Nano Letters, 2007, 7, 2300-2306.	9.1	144
28	Direct detection of E. Coli O157:H7 in selected food systems by a surface plasmon resonance biosensor. LWT - Food Science and Technology, 2007, 40, 187-192.	5.2	143
29	DNAâ~Gold Nanoparticle Reversible Networks Grown on Cell Surface Marker Sites: Application in Diagnostics. ACS Nano, 2011, 5, 2109-2117.	14.6	137
30	In-situ immuno-gold nanoparticle network ELISA biosensors for pathogen detection. International Journal of Food Microbiology, 2013, 164, 70-75.	4.7	136
31	Silver Nanosphere SERS Probes for Sensitive Identification of Pathogens. Journal of Physical Chemistry C, 2010, 114, 16122-16128.	3.1	133
32	Biocompatibility and Biodistribution of Surface-Enhanced Raman Scattering Nanoprobes in Zebrafish Embryos: <i>In vivo</i> and Multiplex Imaging. ACS Nano, 2010, 4, 4039-4053.	14.6	128
33	Biofunctionalized Magnetic Nanoparticle Integrated Mid-Infrared Pathogen Sensor for Food Matrixes. Analytical Chemistry, 2009, 81, 2840-2846.	6.5	127
34	Pulsed UV-light treatment of corn meal for inactivation of Aspergillus niger spores. International Journal of Food Science and Technology, 2003, 38, 883-888.	2.7	124
35	Quantification of Saccharides in Multiple Floral Honeys Using Fourier Transform Infrared Microattenuated Total Reflectance Spectroscopy. Journal of Agricultural and Food Chemistry, 2004, 52, 3237-3243.	5.2	122
36	Nanoantenna array-induced fluorescence enhancement and reduced lifetimes. New Journal of Physics, 2008, 10, 125022.	2.9	112

#	Article	IF	CITATIONS
37	Activity of glucose oxidase functionalized onto magnetic nanoparticles. Biomagnetic Research and Technology, 2005, 3, 1.	2.0	107
38	Inactivation of Staphylococcus aureus by Pulsed UV-Light Sterilization. Journal of Food Protection, 2004, 67, 1027-1030.	1.7	106
39	Highly sensitive fluorescence sensing of zearalenone using a novel aptasensor based on upconverting nanoparticles. Food Chemistry, 2017, 230, 673-680.	8.2	102
40	The electronic tongue and ATR–FTIR for rapid detection of sugars and acids in tomatoes. Sensors and Actuators B: Chemical, 2006, 116, 107-115.	7.8	101
41	Membrane filter-assisted surface enhanced Raman spectroscopy for the rapid detection of E. coli O157:H7 in ground beef. Biosensors and Bioelectronics, 2015, 64, 171-176.	10.1	100
42	Characterization of human breast epithelial cells by confocal Raman microspectroscopy. Cancer Detection and Prevention, 2006, 30, 515-522.	2.1	99
43	SERS aptasensor from nanorod–nanoparticle junction for protein detection. Chemical Communications, 2010, 46, 613-615.	4.1	99
44	Quantitative Evaluation of Sensitivity and Selectivity of Multiplex NanoSPR Biosensor Assays. Biophysical Journal, 2007, 93, 3684-3692.	0.5	97
45	Surface-enhanced Raman spectroscopy at single-molecule scale and its implications in biology. Philosophical Transactions of the Royal Society B: Biological Sciences, 2013, 368, 20120026.	4.0	96
46	Mono and dithiol surfaces on surface plasmon resonance biosensors for detection of Staphylococcus aureus. Sensors and Actuators B: Chemical, 2006, 114, 192-198.	7.8	95
47	Rapid pathogen detection by lateral-flow immunochromatographic assay with gold nanoparticle-assisted enzyme signal amplification. International Journal of Food Microbiology, 2015, 206, 60-66.	4.7	95
48	Rapid detection of foodborne microorganisms on food surface using Fourier transform Raman spectroscopy. Journal of Molecular Structure, 2003, 646, 35-43.	3.6	93
49	Enhancement of single‑photon emission from nitrogen‑vacancy centers with TiN/(Al,Sc)N hyperbolic metamaterial. Laser and Photonics Reviews, 2015, 9, 120-127.	8.7	93
50	Lateral-flow enzyme immunoconcentration for rapid detection of Listeria monocytogenes. Analytical and Bioanalytical Chemistry, 2013, 405, 3313-3319.	3.7	89
51	Analysis of apples varieties – comparison of electronic tongue with different analytical techniques. Sensors and Actuators B: Chemical, 2006, 116, 23-28.	7.8	88
52	Rapid determination of caffeine content in soft drinks using FTIR–ATR spectroscopy. Food Chemistry, 2002, 78, 261-266.	8.2	81
53	A reusable laser wrapped graphene-Ag array based SERS sensor for trace detection of genomic DNA methylation. Biosensors and Bioelectronics, 2017, 92, 755-762.	10.1	81
54	Intracellularly grown gold nanoparticles as potential surface-enhanced Raman scattering probes. Journal of Biomedical Optics, 2007, 12, 020502.	2.6	75

#	Article	IF	CITATIONS
55	Raman Multiplexers for Alternative Gene Splicing. Analytical Chemistry, 2008, 80, 3342-3349.	6.5	75
56	SERS driven cross-platform based multiplex pathogen detection. Sensors and Actuators B: Chemical, 2011, 152, 183-190.	7.8	75
57	An ultrasensitive aptasensor based on fluorescent resonant energy transfer and exonuclease-assisted target recycling for patulin detection. Food Chemistry, 2018, 249, 136-142.	8.2	75
58	Differentiation and detection of microorganisms using Fourier transform infrared photoacoustic spectroscopy. Journal of Molecular Structure, 2002, 606, 181-188.	3.6	73
59	Quantitative Investigation of Compartmentalized Dynamics of ErbB2 Targeting Gold Nanorods in Live Cells by Single Molecule Spectroscopy. ACS Nano, 2009, 3, 4071-4079.	14.6	72
60	Folic Acid Protected Silver Nanocarriers for Targeted Drug Delivery. Journal of Biomedical Nanotechnology, 2012, 8, 751-759.	1.1	72
61	In-situ fluorescent immunomagnetic multiplex detection of foodborne pathogens in very low numbers. Biosensors and Bioelectronics, 2014, 57, 143-148.	10.1	70
62	zNoseâ,,¢ technology for the classification of honey based on rapid aroma profiling. Sensors and Actuators B: Chemical, 2004, 98, 54-62.	7.8	69
63	Adenosine A _{2A} receptors assemble into higherâ€order oligomers at the plasma membrane. FEBS Letters, 2008, 582, 3985-3990.	2.8	69
64	Floral Classification of Honey Using Mid-Infrared Spectroscopy and Surface Acoustic Wave Based z-Nose Sensor. Journal of Agricultural and Food Chemistry, 2005, 53, 6955-6966.	5.2	68
65	Broadband enhancement of spontaneous emission from nitrogen-vacancy centers in nanodiamonds by hyperbolic metamaterials. Applied Physics Letters, 2013, 102, 173114.	3.3	68
66	EZH2 Modifies Sunitinib Resistance in Renal Cell Carcinoma by Kinome Reprogramming. Cancer Research, 2017, 77, 6651-6666.	0.9	66
67	Rheological study of starch and dairy ingredient-based food systems. Food Chemistry, 2004, 86, 571-578.	8.2	64
68	Epigenetic toxicity of PFOA and GenX in HepG2 cells and their role in lipid metabolism. Toxicology in Vitro, 2020, 65, 104797.	2.4	64
69	Diversity of two forms of DNA methylation in the brain. Frontiers in Genetics, 2014, 5, 46.	2.3	63
70	ZnO nanoparticles induced reactive oxygen species promotes multimodal cyto- and epigenetic toxicity. Toxicological Sciences, 2017, 156, kfw252.	3.1	63
71	Measurement of the Attachment and Assembly of Small Amyloid-β Oligomers on Live Cell Membranes at Physiological Concentrations UsingÂSingle-Molecule Tools. Biophysical Journal, 2010, 99, 1969-1975.	0.5	62
72	Mid-IR Biosensor:  Detection and Fingerprinting of Pathogens on Gold Island Functionalized Chalcogenide Films. Analytical Chemistry, 2006, 78, 2500-2506.	6.5	60

#	Article	IF	CITATIONS
73	Protein-directed reduction of graphene oxide and intracellular imaging. Chemical Communications, 2011, 47, 12658.	4.1	60
74	Understanding the Mechanical Properties of DNA Origami Tiles and Controlling the Kinetics of Their Folding and Unfolding Reconfiguration. Journal of the American Chemical Society, 2014, 136, 6995-7005.	13.7	59
75	Alpha Lead Oxide (αâ€₽bO): A New 2D Material with Visible Light Sensitivity. Small, 2018, 14, e1703346.	10.0	58
76	Quantification of 5-methylcytosine, 5-hydroxymethylcytosine and 5-carboxylcytosine from the blood of cancer patients by an enzyme-based immunoassay. Analytica Chimica Acta, 2014, 852, 212-217.	5.4	57
77	Osteosarcoma mechanobiology and therapeutic targets. British Journal of Pharmacology, 2022, 179, 201-217.	5.4	56
78	Simultaneous Monitoring of Organic Acids and Sugars in Fresh and Processed Apple Juice by Fourier Transform Infrared—Attenuated Total Reflection Spectroscopy. Applied Spectroscopy, 2003, 57, 1599-1604.	2.2	55
79	Fluorescence Lifetime Cross Correlation Spectroscopy Resolves EGFR and Antagonist Interaction in Live Cells. Analytical Chemistry, 2010, 82, 6415-6421.	6.5	55
80	Graphene laminated gold bipyramids as sensitive detection platforms for antibiotic molecules. Chemical Communications, 2015, 51, 15494-15497.	4.1	55
81	Detection ofâ€, <i>E. coli</i> â€,O157:H7 from Ground Beef Using Fourier Transform Infrared (FTâ€IR) Spectroscopy and Chemometrics. Journal of Food Science, 2010, 75, M340-6.	3.1	54
82	Application of elastic net and infrared spectroscopy in the discrimination between defective and non-defective roasted coffees. Talanta, 2014, 128, 393-400.	5.5	54
83	Single-Cell Quantification of Cytosine Modifications by Hyperspectral Dark-Field Imaging. ACS Nano, 2015, 9, 11924-11932.	14.6	54
84	Examination of Full Fat and Reduced Fat Cheddar Cheese During Ripening by Fourier Transform Infrared Spectroscopy. Journal of Dairy Science, 1998, 81, 2791-2797.	3.4	53
85	Fourier transform infrared spectroscopy and near infrared spectroscopy for the quantification of defects in roasted coffees. Talanta, 2015, 134, 379-386.	5.5	53
86	Optical Clearing Delivers Ultrasensitive Hyperspectral Dark-Field Imaging for Single-Cell Evaluation. ACS Nano, 2016, 10, 3132-3143.	14.6	52
87	Comparative <i>in vitro</i> toxicity assessment of perfluorinated carboxylic acids. Journal of Applied Toxicology, 2017, 37, 699-708.	2.8	52
88	Magnetic Focus Lateral Flow Sensor for Detection of Cervical Cancer Biomarkers. Analytical Chemistry, 2019, 91, 2876-2884.	6.5	52
89	Gold nanoprobes for theranostics. Nanomedicine, 2011, 6, 1787-1811.	3.3	51
90	Quantitative Surface-Enhanced Raman for Gene Expression Estimation. Biophysical Journal, 2009, 96, 4709-4716.	0.5	50

6

#	Article	IF	CITATIONS
91	Ultrasensitive detection of microbial cells using magnetic focus enhanced lateral flow sensors. Chemical Communications, 2016, 52, 4930-4933.	4.1	50
92	Acute PFOA exposure promotes epigenomic alterations in mouse kidney tissues. Toxicology Reports, 2020, 7, 125-132.	3.3	50
93	Classification of simple and complex sugar adulterants in honey by mid-infrared spectroscopy. International Journal of Food Science and Technology, 2002, 37, 351-360.	2.7	49
94	PCR-Free Quantification of Multiple Splice Variants in a Cancer Gene by Surface-Enhanced Raman Spectroscopy. Journal of Physical Chemistry B, 2009, 113, 14021-14025.	2.6	49
95	Carboxyl-coated magnetic nanoparticles for mRNA isolation and extraction of supercoiled plasmid DNA. Analytical Biochemistry, 2008, 379, 130-132.	2.4	48
96	EFFICACY OF INFRARED HEAT TREATMENT FOR INACTIVATION OF <i>STAPHYLOCOCCUS AUREUS</i> IN MILK. Journal of Food Process Engineering, 2008, 31, 798-816.	2.9	47
97	Epigenetic Editing of Ascl1 Gene in Neural Stem Cells by Optogenetics. Scientific Reports, 2017, 7, 42047.	3.3	45
98	Oxygen nanobubbles revert hypoxia by methylation programming. Scientific Reports, 2017, 7, 9268.	3.3	45
99	Prosperity to challenges: recent approaches in SERS substrate fabrication. Reviews in Analytical Chemistry, 2017, 36, .	3.2	44
100	Fluorescence Lifetime Imaging of Biosensor Peptide Phosphorylation in Single Live Cells. Angewandte Chemie - International Edition, 2013, 52, 3931-3934.	13.8	43
101	Nano/Micro and Spectroscopic Approaches to Food Pathogen Detection. Annual Review of Analytical Chemistry, 2014, 7, 65-88.	5.4	42
102	Oxygen Nanobubble Tracking by Light Scattering in Single Cells and Tissues. ACS Nano, 2017, 11, 2682-2688.	14.6	42
103	Water flattens graphene wrinkles: laser shock wrapping of graphene onto substrate-supported crystalline plasmonic nanoparticle arrays. Nanoscale, 2015, 7, 19885-19893.	5.6	41
104	Determination of cholesterol in dairy products using infrared techniques: 1. FTIR spectroscopy. International Journal of Dairy Technology, 2002, 55, 127-132.	2.8	40
105	Modified graphene oxide sensors for ultra-sensitive detection of nitrate ions in water. Talanta, 2015, 143, 234-239.	5.5	40
106	Plasmonic enhancement in lateral flow sensors for improved sensing of E. coli O157:H7. Biosensors and Bioelectronics, 2019, 126, 324-331.	10.1	40
107	Single Molecule Tools Elucidate H2A.Z Nucleosome Composition. Journal of Cell Science, 2012, 125, 2954-64.	2.0	39
108	Ultrasound beam steering of oxygen nanobubbles for enhanced bladder cancer therapy. Scientific Reports, 2018, 8, 3112.	3.3	39

7

#	Article	IF	CITATIONS
109	Prenatal and ancestral exposure to di(2-ethylhexyl) phthalate alters gene expression and DNA methylation in mouse ovaries. Toxicology and Applied Pharmacology, 2019, 379, 114629.	2.8	39
110	Correct Spectral Conversion between Surfaceâ€Enhanced Raman and Plasmon Resonance Scattering from Nanoparticle Dimers for Singleâ€Molecule Detection. Small, 2013, 9, 1106-1115.	10.0	38
111	Hydrodynamic Size-Dependent Cellular Uptake of Aqueous QDs Probed by Fluorescence Correlation Spectroscopy. Journal of Physical Chemistry B, 2012, 116, 12125-12132.	2.6	37
112	Second Harmonic Super-resolution Microscopy for Quantification of mRNA at Single Copy Sensitivity. ACS Nano, 2014, 8, 12418-12427.	14.6	37
113	Impedimetric detection of bacteria by using a microfluidic chip and silver nanoparticle based signal enhancement. Mikrochimica Acta, 2018, 185, 184.	5.0	37
114	FTIR nanobiosensors for <i>Escherichia coli</i> detection. Beilstein Journal of Nanotechnology, 2012, 3, 485-492.	2.8	36
115	Analysis of potato chips using FTIR photoacoustic spectroscopy. Journal of the Science of Food and Agriculture, 2000, 80, 1805-1810.	3.5	35
116	Aptamer-Mediated Magnetic and Gold-Coated Magnetic Nanoparticles as Detection Assay for Prion Protein Assessment. Biotechnology Progress, 2007, 23, 0-0.	2.6	34
117	Raman Chemical Imaging of Chromate Reduction Sites in a Single Bacterium Using Intracellularly Grown Gold Nanoislands. ACS Nano, 2011, 5, 4729-4736.	14.6	34
118	Surface enhanced Raman spectroscopy (SERS) for the discrimination of Arthrobacter strains based on variations in cell surface composition. Analyst, The, 2012, 137, 4280.	3.5	34
119	Proliferating Cell Nuclear Antigen (PCNA) Is Required for Cell Cycle-regulated Silent Chromatin on Replicated and Nonreplicated Genes. Journal of Biological Chemistry, 2010, 285, 35142-35154.	3.4	33
120	Au nanoparticles on graphitic petal arrays for surface-enhanced Raman spectroscopy. Applied Physics Letters, 2010, 97, 133108.	3.3	33
121	Spectroscopic Differentiation and Quantification of Microorganisms in Apple Juice. Journal of Food Science, 2004, 69, 268-272.	3.1	32
122	Opto-electrokinetic manipulation for high-performance on-chip bioassays. Lab on A Chip, 2012, 12, 4955.	6.0	32
123	Technical advances in global DNA methylation analysis in human cancers. Journal of Biological Engineering, 2017, 11, 10.	4.7	32
124	Single Molecule In Vivo Analysis of Toll-Like Receptor 9 and CpG DNA Interaction. PLoS ONE, 2011, 6, e17991.	2.5	31
125	One-stop genomic DNA extraction by salicylic acid-coated magnetic nanoparticles. Analytical Biochemistry, 2013, 442, 249-252.	2.4	31
126	Laser Shock Tuning Dynamic Interlayer Coupling in Graphene–Boron Nitride Moiré Superlattices. Nano Letters, 2019, 19, 283-291.	9.1	31

#	Article	IF	CITATIONS
127	Surface-Enhanced Raman Imaging of Intracellular Bioreduction of Chromate in Shewanella oneidensis. PLoS ONE, 2011, 6, e16634.	2.5	31
128	Intracellular quantification by surface enhanced Raman spectroscopy. Chemical Physics Letters, 2008, 461, 131-135.	2.6	30
129	Targeted in vivo photodynamic therapy with epidermal growth factor receptor-specific peptide linked nanoparticles. International Journal of Pharmaceutics, 2014, 471, 421-429.	5.2	30
130	The hypomethylating agent Decitabine causes a paradoxical increase in 5-hydroxymethylcytosine in human leukemia cells. Scientific Reports, 2015, 5, 9281.	3.3	30
131	Epigenetic biomarker screening by FLIM-FRET for combination therapy in ER+ breast cancer. Clinical Epigenetics, 2019, 11, 16.	4.1	30
132	Periodic and Dynamic 3-D Gold Nanoparticleâ^'DNA Network Structures for Surface-Enhanced Raman Spectroscopy-Based Quantification. Journal of Physical Chemistry C, 2009, 113, 5980-5983.	3.1	28
133	Dissecting the behavior and function of MBD3 in DNA methylation homeostasis by single-molecule spectroscopy and microscopy. Nucleic Acids Research, 2015, 43, 3046-3055.	14.5	28
134	Inhibition mechanism of green-synthesized copper oxide nanoparticles from <i>Cassia fistula</i> towards <i>Fusarium oxysporum</i> by boosting growth and defense response in tomatoes. Environmental Science: Nano, 2021, 8, 1729-1748.	4.3	28
135	A Study of Alterations in DNA Epigenetic Modifications (5mC and 5hmC) and Gene Expression Influenced by Simulated Microgravity in Human Lymphoblastoid Cells. PLoS ONE, 2016, 11, e0147514.	2.5	28
136	Bimodal counterpropagating-responsive sensing material for the detection of histamine. RSC Advances, 2017, 7, 44933-44944.	3.6	27
137	Studies on Rheological Behaviour of Canola and Wheat. Biosystems Engineering, 1995, 61, 267-274.	0.4	26
138	Effect of PFOA on DNA Methylation and Alternative Splicing in Mouse Liver. Toxicology Letters, 2020, 329, 38-46.	0.8	26
139	Effect of Perfluorooctanoic Acid on the Epigenetic and Tight Junction Genes of the Mouse Intestine. Toxics, 2020, 8, 64.	3.7	25
140	Toward a Mechanistic Understanding of Poly- and Perfluoroalkylated Substances and Cancer. Cancers, 2022, 14, 2919.	3.7	25
141	Study of binding and denaturation dynamics of IgG and anti-IgG using dual color fluorescence correlation spectroscopy. Analytica Chimica Acta, 2008, 625, 103-109.	5.4	24
142	Enhanced Multiphoton Emission from CdTe/ZnS Quantum Dots Decorated on Single-Layer Graphene. Journal of Physical Chemistry C, 2015, 119, 6331-6336.	3.1	24
143	Superplastic Formation of Metal Nanostructure Arrays with Ultrafine Gaps. Advanced Materials, 2016, 28, 9152-9162.	21.0	24
144	PLGA-PEG nano-delivery system for epigenetic therapy. Biomedicine and Pharmacotherapy, 2017, 90, 586-597.	5.6	24

#	Article	IF	CITATIONS
145	Real-time dynamics of methyl-CpG-binding domain protein 3 and its role in DNA demethylation by fluorescence correlation spectroscopy. Epigenetics, 2013, 8, 1089-1100.	2.7	23
146	Multiplex singleâ€cell quantification of rare <scp>RNA</scp> transcripts from protoplasts in a model plant system. Plant Journal, 2017, 90, 1187-1195.	5.7	23
147	Optogenetic regulation of site-specific subtelomeric DNA-methylation. Oncotarget, 2016, 7, 50380-50391.	1.8	23
148	Decitabine Nanoconjugate Sensitizes Human Glioblastoma Cells to Temozolomide. Molecular Pharmaceutics, 2015, 12, 1279-1288.	4.6	22
149	Inside single cells: quantitative analysis with advanced optics and nanomaterials. Wiley Interdisciplinary Reviews: Nanomedicine and Nanobiotechnology, 2015, 7, 387-407.	6.1	22
150	Selective Far Infrared Heating System—Design and Evaluation. I. Drying Technology, 2003, 21, 51-67.	3.1	21
151	Receptor overexpression or inhibition alters cell surface dynamics of EGF–EGFR interaction: New insights from real-time single molecule analysis. Biochemical and Biophysical Research Communications, 2009, 378, 376-382.	2.1	21
152	Innovative Composite Films of Chitosan, Methylcellulose, and Nanoparticles. Journal of Food Science, 2011, 76, N54-60.	3.1	21
153	Intracellularly grown gold nanoislands as SERS substrates for monitoring chromate, sulfate and nitrate localization sites in remediating bacteria biofilms by Raman chemical imaging. Analytica Chimica Acta, 2012, 745, 1-9.	5.4	21
154	Selective increase in subtelomeric DNA methylation: an epigenetic biomarker for malignant glioma. Clinical Epigenetics, 2015, 7, 107.	4.1	21
155	Mitochondrial Dysfunction, Disruption of F-Actin Polymerization, and Transcriptomic Alterations in Zebrafish Larvae Exposed to Trichloroethylene. Chemical Research in Toxicology, 2016, 29, 169-179.	3.3	21
156	A net fishing enrichment strategy for colorimetric detection of E. coli O157:H7. Sensors and Actuators B: Chemical, 2017, 247, 923-929.	7.8	21
157	Colorimetric Detection of Organophosphate Pesticides Based on Acetylcholinesterase and Cysteamine Capped Gold Nanoparticles as Nanozyme. Sensors, 2021, 21, 8050.	3.8	21
158	Ultrasensitive protein detection in blood serum using gold nanoparticle probes by single molecule spectroscopy. Journal of Biomedical Optics, 2009, 14, 040501.	2.6	20
159	High performance immunochromatographic assay combined with surface enhanced Raman spectroscopy. Sensors and Actuators B: Chemical, 2015, 213, 209-214.	7.8	20
160	Exploring the antiâ€quorum sensing activity of a <scp>d</scp> â€limonene nanoemulsion for <i>Escherichia coli</i> O157:H7. Journal of Biomedical Materials Research - Part A, 2018, 106, 1979-1986.	4.0	20
161	Monomeric cohesin state revealed by liveâ€cell singleâ€molecule spectroscopy. EMBO Reports, 2020, 21, e48211.	4.5	20
162	Nano drug delivery systems in upper gastrointestinal cancer therapy. Nano Convergence, 2020, 7, 38.	12.1	20

#	Article	IF	CITATIONS
163	Multifunctional gold nanorod theragnostics probed by multi-photon imaging. European Journal of Medicinal Chemistry, 2012, 48, 330-337.	5.5	19
164	Effect of <scp>T</scp> â€ <scp>DNA</scp> insertions on <scp>mRNA</scp> transcript copy numbers upstream and downstream of the insertion site in <i><scp>A</scp>rabidopsis thaliana</i> explored by surface enhanced <scp>R</scp> aman spectroscopy. Plant Biotechnology Journal, 2014, 12, 568-577.	8.3	19
165	Bioinspired glycosaminoglycan hydrogels via click chemistry for 3D dynamic cell encapsulation. Journal of Applied Polymer Science, 2019, 136, 47212.	2.6	19
166	Nanoscale histone localization in live cells reveals reduced chromatin mobility in response to DNA damage. Journal of Cell Science, 2014, 128, 599-604.	2.0	18
167	Detection and quantification of alternative splice sites in Arabidopsis genes AtDCL2 and AtPTB2 with highly sensitive surface enhanced Raman spectroscopy (SERS) and gold nanoprobes. FEBS Letters, 2014, 588, 1637-1643.	2.8	18
168	Epigenetic Modifications, and Alterations in Cell Cycle and Apoptosis Pathway in A549 Lung Carcinoma Cell Line upon Exposure to Perfluoroalkyl Substances. Toxics, 2020, 8, 112.	3.7	18
169	Multi and transgenerational epigenetic effects of di-(2-ethylhexyl) phthalate (DEHP) in liver. Toxicology and Applied Pharmacology, 2020, 402, 115123.	2.8	18
170	Rapid evaluation and discrimination of γ-irradiated carbohydrates using FT-Raman spectroscopy and canonical discriminant analysis. Journal of the Science of Food and Agriculture, 2007, 87, 1244-1251.	3.5	17
171	Perfluorooctanoic acid (PFOA) exposure inhibits DNA methyltransferase activities and alters constitutive heterochromatin organization. Food and Chemical Toxicology, 2020, 141, 111358.	3.6	17
172	Per- and Polyfluoroalkyl Substance Exposure Combined with High-Fat Diet Supports Prostate Cancer Progression. Nutrients, 2021, 13, 3902.	4.1	17
173	An integrated microsystem with dielectrophoresis enrichment and impedance detection for detection of Escherichia coli. Biomedical Microdevices, 2017, 19, 34.	2.8	16
174	Toxicological effects of trichloroethylene exposure on immune disorders. Immunopharmacology and Immunotoxicology, 2017, 39, 305-317.	2.4	16
175	Point-of-care test for cervical cancer in LMICs. Oncotarget, 2016, 7, 18787-18797.	1.8	16
176	Determination of cholesterol in dairy products by infrared techniques: 2. FT-NIR method. International Journal of Dairy Technology, 2002, 55, 133-138.	2.8	15
177	Single molecule Raman spectroscopic assay to detect transgene from GM plants. Analytical Biochemistry, 2017, 532, 60-63.	2.4	14
178	A hybrid FLIM-elastic net platform for label free profiling of breast cancer. Analyst, The, 2013, 138, 7127.	3.5	13
179	PFOA induces alteration in DNA methylation regulators and SARS-CoV-2 targets Ace2 and Tmprss2 in mouse lung tissues. Toxicology Reports, 2021, 8, 1892-1898.	3.3	13
180	Rational Design of Surface-State Controlled Multicolor Cross-Linked Carbon Dots with Distinct Photoluminescence and Cellular Uptake Properties. ACS Applied Materials & Interfaces, 2021, 13, 59747-59760.	8.0	13

#	Article	IF	CITATIONS
181	Nanostructured thin films as surfaceâ€enhanced Raman scattering substrates. Journal of Raman Spectroscopy, 2013, 44, 35-40.	2.5	12
182	Second harmonic generation correlation spectroscopy for single molecule experiments. Optics Express, 2013, 21, 27063.	3.4	12
183	Trichloroethylene sensing in water based on SERS with multifunctional Au/TiO ₂ core–shell nanocomposites. Analyst, The, 2015, 140, 6625-6630.	3.5	12
184	Filtrationâ€Assisted Fabrication of Largeâ€Area Uniform and Longâ€Term Stable Graphene Isolated Nanoâ€Ag Array Membrane as Surface Enhanced Raman Scattering Substrate. Advanced Materials Interfaces, 2018, 5, 1701221.	3.7	12
185	Enhanced Energy Transfer from Nitrogenâ€Vacancy Centers to Threeâ€Dimensional Graphene Heterostructures by Laser Nanoshaping. Advanced Optical Materials, 2021, 9, 2001830.	7.3	12
186	Differentiation of cancer cells in two-dimensional and three-dimensional breast cancer models by Raman spectroscopy. Journal of Biomedical Optics, 2013, 18, 117008.	2.6	11
187	Kinase phosphorylation monitoring with i-motif DNA cross-linked SERS probes. Chemical Communications, 2016, 52, 410-413.	4.1	11
188	Nanovaccine for Plants from Organic Waste: <scp>d</scp> -Limonene-Loaded Chitosan Nanocarriers Protect Plants against <i>Botrytis cinerea</i> . ACS Sustainable Chemistry and Engineering, 2021, 9, 9903-9914.	6.7	11
189	Paper-Based Test for Rapid On-Site Screening of SARS-CoV-2 in Clinical Samples. Biosensors, 2021, 11, 488.	4.7	11
190	Nephrotoxicity of perfluorooctane sulfonate (PFOS)—effect on transcription and epigenetic factors. Environmental Epigenetics, 2022, 8, .	1.8	11
191	Rapid Estimation of pol content in sugarcane juice using FTIR-ATR spectroscopy. Sugar Tech, 2003, 5, 143-148.	1.8	10
192	Quantification of receptor targeting aptamer binding characteristics using singleâ€molecule spectroscopy. Biotechnology and Bioengineering, 2011, 108, 1222-1227.	3.3	10
193	A native chromatin extraction method based on salicylic acid coated magnetic nanoparticles and characterization of chromatin. Analyst, The, 2015, 140, 938-944.	3.5	10
194	Epigenetic toxicity of trichloroethylene: a single-molecule perspective. Toxicology Research, 2016, 5, 641-650.	2.1	10
195	Monitoring focal adhesion kinase phosphorylation dynamics in live cells. Analyst, The, 2017, 142, 2713-2716.	3.5	10
196	Real-Time Multiplex Kinase Phosphorylation Sensors in Living Cells. ACS Sensors, 2017, 2, 1225-1230.	7.8	10
197	Copper mediates mitochondrial biogenesis in retinal pigment epithelial cells. Biochimica Et Biophysica Acta - Molecular Basis of Disease, 2020, 1866, 165843.	3.8	10
198	Hormesis-Inducing Essential Oil Nanodelivery System Protects Plants against Broad Host-Range Necrotrophs. ACS Nano, 2021, 15, 8338-8349.	14.6	10

#	Article	IF	CITATIONS
199	Dextran-Based Oxygen Nanobubbles for Treating Inner Retinal Hypoxia. ACS Applied Nano Materials, 2021, 4, 6583-6593.	5.0	10
200	Hyperspectral dark-field microscopy for pathogen detection based on spectral angle mapping. Sensors and Actuators B: Chemical, 2022, 367, 132042.	7.8	10
201	Spectroscopic Quantification of Bacteria Using Artificial Neural Networks. Journal of Food Protection, 2004, 67, 2550-2554.	1.7	9
202	Fast aroma profiling to detect invert sugar adulteration with zNose?. Journal of the Science of Food and Agriculture, 2005, 85, 243-250.	3.5	9
203	Pathogen Sensors. Sensors, 2009, 9, 8610-8612.	3.8	9
204	Probing site-exclusive binding of aqueous QDs and their organelle-dependent dynamics in live cells by single molecule spectroscopy. Analyst, The, 2013, 138, 2871.	3.5	9
205	Quantitative real-time kinetics of optogenetic proteins CRY2 and CIB1/N using single-molecule tools. Analytical Biochemistry, 2014, 458, 58-60.	2.4	9
206	Beyond quantification: <i>in situ</i> analysis of transcriptome and preâ€ <scp>mRNA</scp> alternative splicing at the nanoscale. Wiley Interdisciplinary Reviews: Nanomedicine and Nanobiotechnology, 2017, 9, e1443.	6.1	9
207	Chromosome loading of cohesin depends on conserved residues in Scc3. Current Genetics, 2021, 67, 447-459.	1.7	9
208	Multi-layered alginate hydrogel structures and bacteria encapsulation. Chemical Communications, 2022, 58, 8584-8587.	4.1	9
209	Dynamic Heterochromatin States in Anisotropic Nuclei of Cells on Aligned Nanofibers. ACS Nano, 2022, 16, 10754-10767.	14.6	9
210	Quantifying the local density of optical states of nanorods by fluorescence lifetime imaging. New Journal of Physics, 2014, 16, 063069.	2.9	8
211	The transition structure of chromatin fibers at the nanoscale probed by cryogenic electron tomography. Nanoscale, 2019, 11, 13783-13789.	5.6	8
212	Nanoscale histone localization in live cells reveals reduced chromatin mobility in response to DNA damage. Development (Cambridge), 2015, 142, e0407-e0407.	2,5	8
213	Non-fluorescent quantification of single mRNA with transient absorption microscopy. Nanoscale, 2016, 8, 19242-19248.	5.6	7
214	Epigenetic Process Monitoring in Live Cultures with Peptide Biosensors. ACS Sensors, 2019, 4, 562-565.	7.8	7
215	Multiplexable fluorescence lifetime imaging (FLIM) probes for Abl and Src-family kinases. Chemical Communications, 2020, 56, 13409-13412.	4.1	7
216	16S rRNA Monitoring Point-of-Care Magnetic Focus Lateral Flow Sensor. ACS Omega, 2021, 6, 11095-11102.	3.5	7

#	Article	IF	CITATIONS
217	Early postnatal exposure to di(2-ethylhexyl) phthalate causes sex-specific disruption of gonadal development in pigs. Reproductive Toxicology, 2021, 105, 53-61.	2.9	7
218	Regulatory landscape and clinical implication of MBD3 in human malignant glioma. Oncotarget, 2016, 7, 81698-81714.	1.8	7
219	ESTIMATION Of PARTICLE SIZE bY DRIFTS and FTIR-PAS. Particulate Science and Technology, 1999, 17, 269-282.	2.1	5
220	Selective Far Infrared Heating System—Spectral Manipulation. II. Drying Technology, 2003, 21, 69-82.	3.1	5
221	Single-cell screening and quantification of transcripts in cancer tissues by second-harmonic generation microscopy. Journal of Biomedical Optics, 2015, 20, 096016.	2.6	5
222	Cross-platform detection of epigenetic modifications from extracted chromatin in leucocytes from blood. Analytical Chemistry Research, 2015, 4, 39-44.	2.0	5
223	Modulation of Gene Silencing by Cdc7p via H4 K16 Acetylation and Phosphorylation of Chromatin Assembly Factor CAF-1 in <i>Saccharomyces cerevisiae</i> . Genetics, 2019, 211, 1219-1237.	2.9	5
224	Chromatin hierarchical branching visualized at the nanoscale by electron microscopy. Nanoscale Advances, 2021, 3, 1019-1028.	4.6	5
225	Checkpoint enrichment for sensitive detection of target bacteria from large volume of food matrices. Analytica Chimica Acta, 2020, 1127, 114-121.	5.4	4
226	Hypoxia Re-Programming Oxygen Nanobubbles Sensitize Human Glioblastoma Cells to Temozolomide via Methylation Alterations. Journal of Bionanoscience, 2017, 11, 337-345.	0.4	4
227	Applications of Raman Spectroscopy for Food Quality Measurement. , 0, , 143-163.		3
228	Latest Developments of Nanotoxicology in Plants. , 2015, , 125-151.		3
229	CAF-1 and Rtt101p function within the replication-coupled chromatin assembly network to promote H4 K16ac, preventing ectopic silencing. PLoS Genetics, 2020, 16, e1009226.	3.5	3
230	SERS in Salt Wells. ChemPhysChem, 2009, 10, 2670-2673.	2.1	2
231	Gene Expression Analysis Using Conventional and Imaging Methods. , 2013, , 141-162.		2
232	Basic studies on epigenetic carcinogenesis of low-dose exposure to 1-trichloromethyl-1,2,3,4-tetrahydro-β-carboline (TaClo) in vitro. PLoS ONE, 2017, 12, e0172243.	2.5	2
233	Rapid and unbiased extraction of chromatin associated RNAs from purified native chromatin. Journal of Chromatography A, 2015, 1426, 64-68.	3.7	1
234	Cover Image, Volume 9, Issue 4. Wiley Interdisciplinary Reviews: Nanomedicine and Nanobiotechnology, 2017, 9, e1484.	6.1	1

#	Article	IF	CITATIONS
235	Understanding the dynamics and structure of epigenetic states with single-molecule fluorescence microscopy. Current Opinion in Biomedical Engineering, 2019, 12, 18-24.	3.4	1
236	Application of an Optically Induced Electrokinetic Manipulation Technique on Live Bacteria. , 2010, , .		1
237	Optical Microscopy and Spectroscopy for Epigenetic Modifications in Single Living Cells. Methods in Pharmacology and Toxicology, 2017, , 135-154.	0.2	1
238	Sensitivity and Selectivity Limits of Multiplex NanoSPR Biosensor Assays. ACS Symposium Series, 2008, , 386-401.	0.5	0
239	mRNA quantification via second harmonic super resolution microscopy. , 2014, , .		0
240	Quantifying local density of optical states of nanorods by fluorescence lifetime imaging. Proceedings of SPIE, 2014, , .	0.8	0
241	Surface-enhanced Raman spectroscopy for cancer characterization. , 2022, , 373-393.		0
242	Epigenetic alterations associated with dexamethasone sodium phosphate through DNMT and TET in RPE cells Molecular Vision, 2021, 27, 643-655.	1.1	0